Final Report for MEng Individual Project

Mathematical modelling of fungal growth *in vitro*

Author Name: Joshua Sia

CID: 01412775

Supervisors: Dr Reiko Tanaka, Tara Hameed

Submitted in partial fulfilment of the requirements for the award of MEng in Biomedical Engineering from Imperial College London

June 2021 **Word Count:** 3583

Acknowledgements

First and foremost, I would like to thank my supervisors, Dr Reiko Tanaka and Ms Tara Hameed, for providing me with the opportunity to explore my interests, as well as for the support and guidance I received throughout the project.

To my friends and family, thank you for making me happy everyday.

Abstract

Background Invasive aspergillosis (IA) is a pulmonary disease with a high mortality rate and a high rate of treatment failure. In humans, the most common pathogen of IA is *A. fumigatus*, however, the virulence factors responsible are insufficiently understood from a quantitative perspective. Previous studies have demonstrated a correlation between germination rates and prevalence of opportunistic pathogens among different *Aspergillus* species, however, a study on hyphal growth rates has not been performed before.

Methods Mixed effects exponential and logistic growth models were used to estimate the growth rates of *Aspergillus* growth and significance testing was performed.

Results No significant difference (p=0.15) was found for *A. fumigatus* growth with and without epithelial cells. Furthermore, the maximal growth rates of all 3 fungal species used in the study were significantly different from one another at the Bonferroni corrected 0.05 significance level, with that of *A. fumigatus* being the largest (43.39±2.92 for *A. fumigatus*, 8.09 ± 1.05 for *A. tubingensis* and 6.95 ± 0.91 for *A. niger*).

Conclusion Mixed effects growth models were successfully developed which consistently had lower information criteria values and cross validation errors than the complete pooling model, suggesting that the mixed effects model has better generalisation for datasets involving inherent groupings. Results corresponding to *A. fumigatus* grown with and without epithelial cells imply that epithelial cells only have an impact on condia germination, but not on hyphal growth. Additionally, *A. fumigatus* has the highest maximal growth rate among the three species studied which implies that the maximum growth rate is a virulence factor indicative of prevalence in IA.

Contents

1 Introduction

1.1 Background

Invasive aspergillosis (IA) is an acute pulmonary disease that develops when conidia, or spores, produced by *Aspergillus* fungi are inhaled [1][2]. It typically occurs in immunocompromised patients, such as neutropenic patients undergoing chemotherapy for cancer [3][4]. However, recent studies have found that non-immunocompromised patients with underlying respiratory diseases such as COPD or cystic fibrosis are also susceptible to developing IA [5][6].

Patients suffering from IA experience variable and non-specific symptoms such as fever, chest pain, cough, and shortness of breath which make the diagnosis of IA challenging [2]. Even when IA is diagnosed and treated, high mortality rates are still observed, reaching up to 86% and 90% in neutropenic and leukemia patients respectively, with death occurring within 14 to 21 days [3][7]. Due to the difficulties in diagnosing IA and the rapid progression of the disease, clinicians often treat patients before a clear diagnosis is established. Currently, most IA treatments involve the use of anti-fungal drugs such as azoles and amphotericin B formulations which are either taken orally or intravenously [8]. Newer treatment strategies such as combination therapy and immunotherapy are also being developed, however, there is a lack of controlled clinical trials and these methods remain understudied [9].

In humans, the most common pathogen of IA is the fungal species *Aspergillus fumigatus* [10]. *A. fumigatus* is a common fungus found in plants, soil and food items. It is characterised by a high sporulating capacity which results in high concentrations of conidia in the air, and an ability to thrive in a variety of temperatures, pH, and oxygen concentrations [11]. Furthermore, *A. fumigatus* also has sophisticated mechanisms to acquire nutrients such as carbon and nitrogen in the human body, which allow *Aspergillus* fungi and in particular *A. fumigatus* to become a successful virulent pathogen [9].

Pulmonary epithelial cells (ECs) play an important role in combating IA since it is the first line of host defence and it acts as an extension to the immune system. When conidia are inhaled by healthy individuals, they are usually eliminated through mucociliary clearance by the bronchial ECs. However, some conidia can reach the alveolar ECs, where they are phagocytosed by macrophages and are destroyed by lysosomes. ECs also produce cytokines and chemokines that activate the immune system, and employ neutrophils which use reactive oxygen species dependent mechanisms to clear the fungal infection [9][12][13]. A lack of any of these defence mechanisms in immunocompromised patients, or patients with respiratory diseases may allow the inhaled conidia to germinate into hyphae. Rapid hyphal growth then results in pulmonary damage, which can lead to respiratory failure and death [7].

1.2 Motivation

Although newer and more effective antifungal drugs are being developed, current antifungal treatments still have a high failure rate (75-85%) which is partly due to patients being unable to tolerate high dosages of the drugs [1][8]. Maschmeyer et al. (2007) reported that among 201 neutropenic or transplant patients, up to 31% of patients have discontinued anti-fungal therapies due to adverse effects such as fever, shortness of breath, and toxicity [8]. In recent years, several *Aspergillus* fungi have also shown resistance to the drugs used in IA treatments [14]. In short, there is a need for better methods to treat IA successfully.

A. fumigatus is the most prevalent species in IA, however, the virulence factors responsible still remain understudied quantitatively under a robust framework. Additionally, there is no standard growth metric used to measure fungal growth, and many different metrics such as hyphal tip extension, colony radius, biomass, etc. are used which focus on growth at different levels of the fungi, from individual hyphae to populations of fungal networks [11][15]. The prevalence of *A. fumigatus* explained by hyphal length as a virulence factor thus warrants further investigation.

Araujo et al. (2004) showed a direct correlation between germination rates and prevalence of opportunistic pathogens among different *Aspergillus* species [16]. Additionally, Paisley et al. (2005) also found a direct correlation between fungal growth rates and virulence among nine *A. fumigatus* isolates [17]. These studies imply that therapies lowering the fungal germination or growth rate may be effective at decreasing fungal burden and in consequence, lower the mortality rate [11]. The study conducted by Araujo et al. was focused only on germination rates, while Paisley et al. focused on different *A. fumigatus* isolates. To expand on this research, this study aims to quantitatively measure and compare hyphal growth rates as a virulence factor across multiple *Aspergillus* strains and species, and study the correlation between hyphal growth rates and virulence across multiple *Aspergillus* strains and species. A better understanding of the relationship between hyphal growth and virulence can potentially lead to the development of targeted therapies, which may reduce the drug dosage required in less virulent IA-causing species, and result in more effective combination therapies specific to the invasive fungal species.

Studying the effects of ECs on fungal growth also has implications for future fungal therapies such as immunotherapeutic treatment strategies. Richard et al. (2018) demonstrated that bronchial ECs inhibit *A. fumigatus* conidia germination and play an active role in the phagocytosis of conidia [18]. ECs also produce cytokines and chemokines which activate the immune system in response to hyphal growth [13]. However, there are no previous studies analysing the hyphal length of *Aspergillus* grown with ECs. By studying the effects ECs have on hyphal growth rates quantitatively, the viability and effectiveness of immunotherapies such as cytokine therapy on hyphal

growth can be better understood [19].

1.3 Aims and Objectives

The aims of this study are to: (i) Investigate why *A. fumigatus* is the most prevalent species in IA by using growth rates as a virulence factor, (ii) Perform a robust comparative analysis of the hyphal growth rates of different *Aspergillus* strains and species (iii) Study the relationship between hyphal growth rates and virulence across multiple *Aspergillus* strains and species, and (iv) Explore the effects of ECs on the hyphal growth rates of *A. fumigatus*.

In order to achieve these aims, the objectives of this study are to: (i) Propose fundamental mathematical models of *Aspergillus* hyphal growth, (ii) Compare the models using state-of-the-art model selection tools, (iii) Compare the hyphal growth rates of different *Aspergillus* strains and species and perform a rank correlation test to determine whether there is a correlation between hyphal growth rates and virulence, and (iv) Compare the hyphal growth rates of *A. fumigatus* grown with and without ECs.

2 Experimental Data

The study is conducted on two sets of data collected by experimental collaborators from the Manchester Fungal Infection Group (MFIG). The first data set corresponds to *A. fumigatus* growth with and without ECs. The fungi were all grown on fungal RPMI medium under the same experimental setup. There are 15 experimental repeats for *A. fumigatus* grown with ECs and 10 experimental repeats for *A. fumigatus* grown without ECs. The growth metric used is the length of the main hyphal branch in μm and it is measured every hour until the single hyphae can no longer be tracked due to overcrowding (Figure 2.1).

The second data set corresponds to the growth data of 11 *Aspergillus* strains which are subtypes of 3 *Aspergillus* species, namely *A. fumigatus*, *A. niger*, and *A. tubingensis* (Figure 2.2, Appendix A). All the *Aspergillus* strains were grown on fungal RPMI and 10-15 experimental repeats were performed for each fungal strain. The growth metric used is also the length of the main hyphal branch in μm and it is measured every hour until the single hyphae can no longer be tracked due to overcrowding.

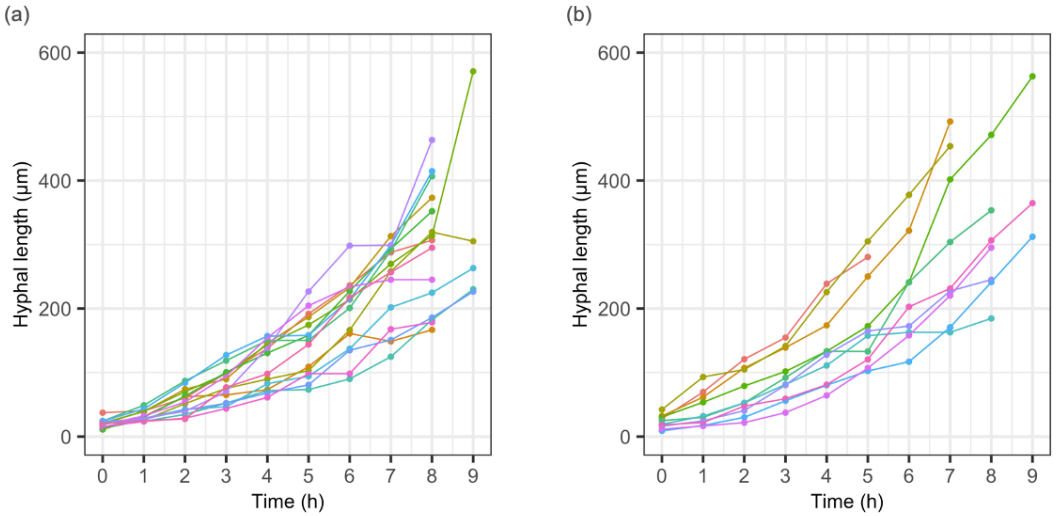

Figure 2.1: *A. fumigatus* growth (a) with ECs and (b) without ECs measured using the hyphal length

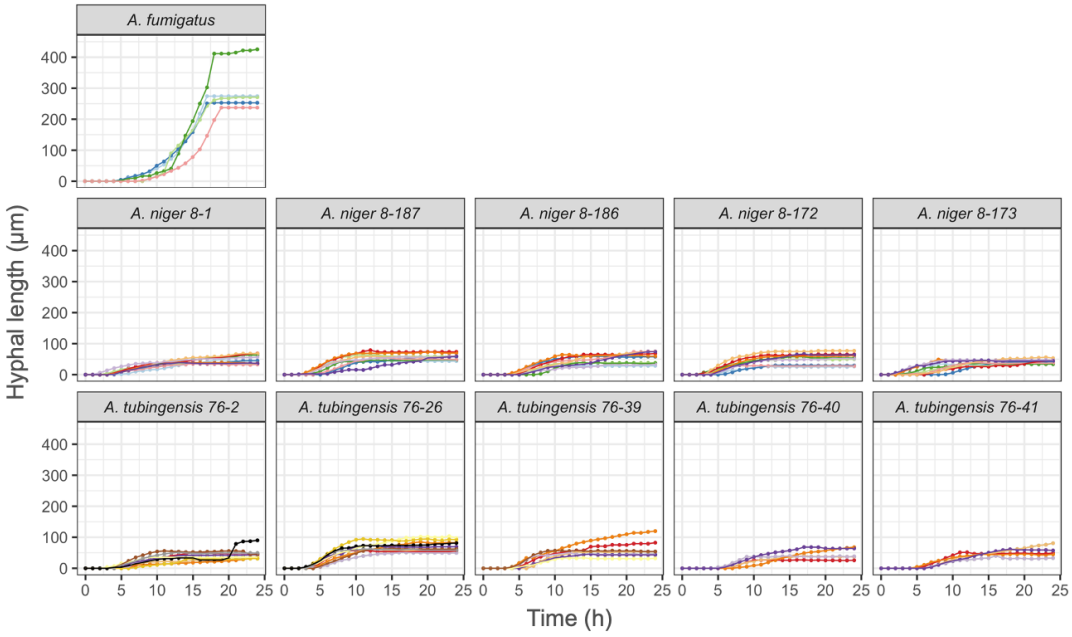

Figure 2.2: Growth of 11 *Aspergillus* strains measured using the hyphal length. There is 1 strain for *A. fumigatus*, 5 strains for *A. niger* and 5 strains for *A. tubingensis*.

3 Methods

The modelling workflow is outlined below in Figure 3.1. The model is trained on the data and is evaluated using various model selection tools.

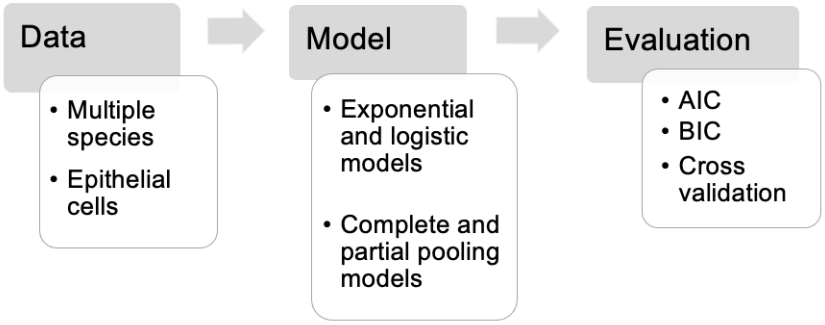

Figure 3.1: Modelling workflow

3.1 Growth models

Two growth models are explored in this study which correspond to an exponential growth model and a logistic growth model. The exponential growth model was used for the dataset describing *A. fumigatus* grown with and without ECs because it is a simple model with only 2 parameters, and data visualisation revealed exponential growth with no asymptote. On the other hand, the logistic growth model was used for the dataset involving multiple *Aspergillus* strains since it only has 3 parameters, and there is an asymptote to growth. A model with a higher number of parameters may result in a better fit, however, it is more likely to overfit to noise in the data as well which leads to poor generalisation.

A Exponential growth model

The exponential growth model has two parameters for the y-intercept A, and the growth rate B, and it is used to explore the effects of ECs on hyphal growth rates.

$$\hat{y}(x) = A\mathrm{e}^{Bx} \tag{1}$$

B Logistic growth model

The logistic growth model has three parameters for the asymptote A, the inflection point B, and the inverse of the slope C (Figure 3.2).

$$\hat{y}(x) = \frac{A}{1 + \mathrm{e}^{\frac{B-x}{C}}} \tag{2}$$

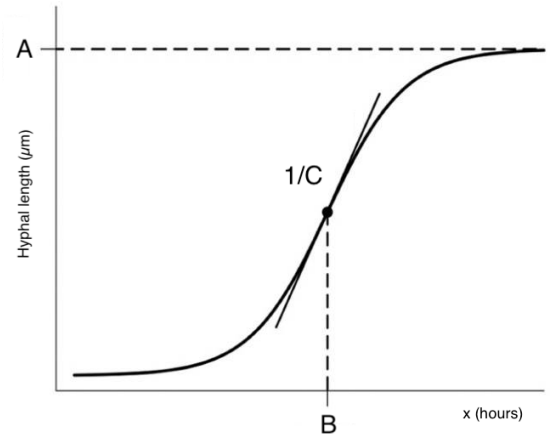

Figure 3.2: The logistic growth model [20]

The derivative of the logistic model describes the growth rate at each time point x where $z = \exp\left(\frac{B-x}{C}\right)$.

$$\frac{d\hat{y}}{dx} = \frac{A}{C}\frac{z}{(1+z)^2} \tag{3}$$

To find the maximal growth rate, the expression for the derivative is evaluated at the inflection point $x = B$.

$$\frac{d\hat{y}}{dx}\Big|_{x=B} = \frac{A}{4C} \tag{4}$$

The standard deviation of the maximal growth rate is then given by

$$\sigma_d = \frac{d}{4}\sqrt{\left(\frac{\sigma_A}{A}\right)^2 + \left(\frac{\sigma_C}{C}\right)^2} \tag{5}$$

3.2 Pooling models

A consideration to take into account when modelling is how inherent groupings in the data, such as experimental replicates, should be dealt with since it is likely that data points originating from the same group will be more correlated. A complete pooling (CP) model assumes that there are no significant differences across the different groups. Thus, data from all the groups are pooled together and a single regression is performed over all the data points (Equation 6).

$$y_i = A\mathrm{e}^{Bx} + \epsilon_i \tag{6}$$

On the other hand, a mixed effects model (MEM), also called a partial pooling model, has fixed effects parameters which account for growth trends at the population level, and random effects parameters which account for variations in growth between smaller groups such as replicates (Equation 7). y_{ij} is the hyphal length in μm for the i^{th} observation of the j^{th} group, A and B are the fixed effects parameters, a_j and b_j are the random effects parameters for the j^{th} group, x is the time in hours, and ϵ describes the noise.

$$y_{ij} = (A + a_j) + \mathrm{e}^{(B+b_j)x} + \epsilon_{ij} \tag{7}$$

$$a_j \sim N(0, \sigma_a^2)$$

$$b_j \sim N(0, \sigma_b^2) \tag{8}$$

It is known a priori for the second data set that there are multiple inherent groupings in the data, namely (i) the genus *Aspergillus* as a whole, (ii) different species in the genus, (iii) different strains in the species, and finally (iv) replicates in the strains. To account for all the groupings in the data, a multilevel mixed effects model is used with 4 levels. The levels describe the nesting of groups in the data (Figure 3.3). For the logistic model, the multilevel mixed effects model is as follows where l represents the time point in a replicate, k represents the replicates, j represents the strains, and i represents the species (Equation 9).

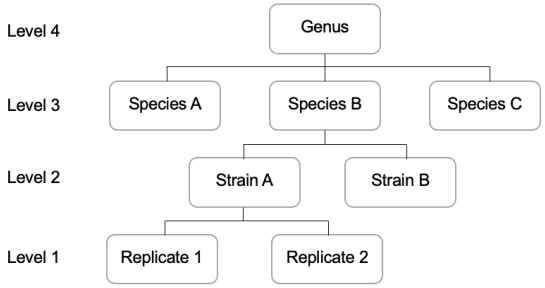

Figure 3.3: Multilevel mixed effects model with 4 levels

$$\text{Level 1} : \hat{y}_{ijkl}(x) = \frac{A_{ijk}}{1 + \mathrm{e}^{\frac{B_{ijk}-x}{C_{ijk}}}} + \epsilon_{ijkl}$$

$$\begin{aligned}
\text{Level 2} : A_{ijk} &= A_{ij} + u_{ijk}\,, \quad u_{ijk} \sim \mathcal{N}(0, \sigma_u^2) \\
B_{ijk} &= B_{ij} + v_{ijk}\,, \quad v_{ijk} \sim \mathcal{N}(0, \sigma_v^2) \\
C_{ijk} &= C_{ij} + w_{ijk}\,, \quad w_{ijk} \sim \mathcal{N}(0, \sigma_w^2)
\end{aligned}$$

$$\begin{aligned}
\text{Level 3} : A_{ij} &= A_i + \bar{u}_{ij}\,, \quad \bar{u}_{ij} \sim \mathcal{N}(0, \sigma_{\bar{u}}^2) \\
B_{ij} &= B_i + \bar{v}_{ij}\,, \quad \bar{v}_{ij} \sim \mathcal{N}(0, \sigma_{\bar{v}}^2) \\
C_{ij} &= C_i + \bar{w}_{ij}\,, \quad \bar{w}_{ij} \sim \mathcal{N}(0, \sigma_{\bar{w}}^2)
\end{aligned}$$

$$\begin{aligned}
\text{Level 4} : A_i &= A_0 + \tilde{u}_i\,, \quad \tilde{u}_i \sim \mathcal{N}(0, \sigma_{\tilde{u}}^2) \\
B_i &= B_0 + \tilde{v}_i\,, \quad \tilde{v}_i \sim \mathcal{N}(0, \sigma_{\tilde{v}}^2) \\
C_i &= C_0 + \tilde{w}_i\,, \quad \tilde{w}_i \sim \mathcal{N}(0, \sigma_{\tilde{w}}^2)
\end{aligned} \tag{9}$$

A_0, B_0 and C_0 are the fixed effects which account for growth trends at the *Aspergillus* genus level. The random effects are captured by the variables σ_u, $\sigma_{\bar{u}}$, $\sigma_{\tilde{u}}$, σ_v, $\sigma_{\bar{v}}$, $\sigma_{\tilde{v}}$, σ_w, $\sigma_{\bar{w}}$, and $\sigma_{\tilde{w}}$.

3.3 Noise models

It is equally important to consider how noise should be accounted for in the model. An additive noise model assumes a constant level of noise regardless of the model prediction $\hat{y}$ (Equation 10) whereas a multiplicative noise model assumes that the noise increases as the model prediction $\hat{y}$ increases (Equation 11). It is assumed that noise is independent and identically distributed.

$$y \sim \mathcal{N}\left(\hat{y}, \sigma^2\right) \tag{10}$$

$$\log(y) \sim \mathcal{N}\left(\log\left(\hat{y}\right), \sigma^2\right) \tag{11}$$

Additive noise may correspond to the random errors that are made during measurement of the hyphal length, while multiplicative noise might occur when the hyphal branch grows in or out of the 2D plane, or when it doesn't grow in a straight line, causing the measurement error to increase as the hyphal length increases.

3.4 Evaluation

In order to identify the optimal model, information criteria values, namely the AIC and BIC, and cross validation were used. Three metrics for model selection are computed because the results of one metric may not be accurate, and optimising for one metric is also a form of overfitting.

The AIC and BIC reward a better fit to the data through the maximum likelihood value of the model $\hat{L}$, and penalise overfitting through the number of model parameters k and number of data points n. The BIC penalises an increase in the number of model parameters more heavily than the AIC. A lower information criteria value indicates a better model.

$$\text{AIC} = -2\ln(\hat{L}) + 2k \tag{12}$$

$$\text{BIC} = -2\ln(\hat{L}) + k\ln(n) \tag{13}$$

Similarly, cross validation (CV) can be used to estimate the out-of-sample prediction error by first training the model on a training set, and then evaluating the error on a testing set. In k-fold CV, the data set is split into k sub-samples, each with n/k samples, where n is the number of data points (Figure 3.4). At each iteration, the model is trained on the training set, and the mean squared error (MSE) between the model prediction and the testing set is computed. The final CV error is the mean of the MSE over all the iterations.

For the dataset describing *A. fumigatus* grown with and without ECs, CV was performed over replicates, in order to obtain the generalisation error to a new set of experimental data. On the other hand, for the dataset involving multiple *Aspergillus* strains, CV was performed over strains to obtain the generalisation error when predicting growth trends of a new strain.

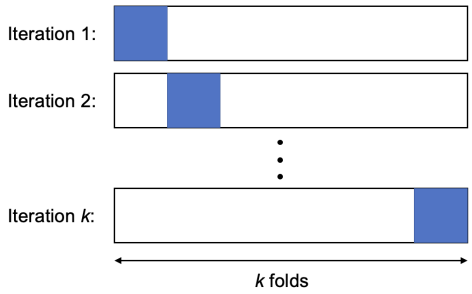

Figure 3.4: Illustration of k-fold cross validation. The blue area represents the testing set, and the white area represents the training set.

4 Results

4.1 Effect of ECs on hyphal growth

Since the complete pooling model performs a single regression, the model does not fit well to certain experimental replicates (Figure 4.1). As a result, the complete pooling model resulted in higher information criteria values than the mixed effects model for both noise models which implies worse generalisation (Table 4.1). Growth rates from the mixed effects models were then used to study the effects of ECs on hyphal growth.

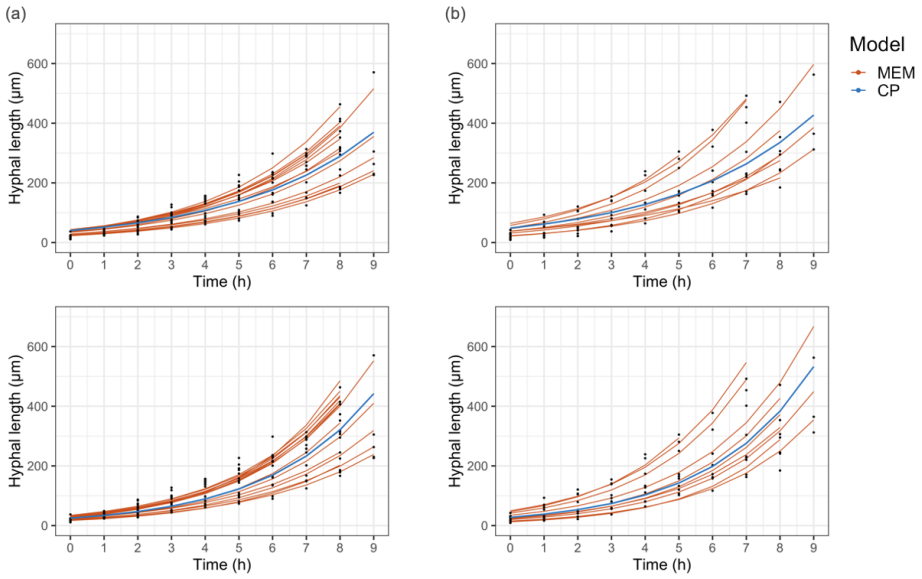

Figure 4.1: Fits of the CP and MEM models for *A. fumigatus* growth (a) with ECs and (b) without ECs for (top) additive noise and (bottom) multiplicative noise

Table 4.1: Comparison between information criteria of four exponential models. The CV error is reported with its standard deviation. $^{1}\times 10^{4}$ for additive noise models.

Model	AIC	BIC	CV error[1]
CP - Additive noise	1123.7	1129.5	3.18 ± 2.11
MEM - Additive noise	**870.7**	**885.4**	3.00 ± 1.45
CP - Multiplicative noise	1051.6	1057.5	1.32 ± 0.47
MEM - Multiplicative noise	**851.4**	**866.1**	1.33 ± 0.58

No significant difference was found at the 0.05 significance level for *A. fumigatus* grown with and without epithelial cells for either the additive or multiplicative noise mixed effects models (Table 4.2, Figure 4.2) which suggests that ECs do not have an effect on *A. fumigatus* growth. However, complex interactions in the body involving ECs may not be captured by *in vitro* experiments why is possibly why no significance was found.

Table 4.2: Comparison between growth rates of *A. fumigatus* grown with and without epithelial cells with the 95% confidence intervals.

Model	**With ECs**	**Without ECs**	p-value
Additive noise MEM	0.267 ± 0.018	0.285 ± 0.030	0.31
Multiplicative noise MEM	0.327 ± 0.022	0.353 ± 0.028	0.15

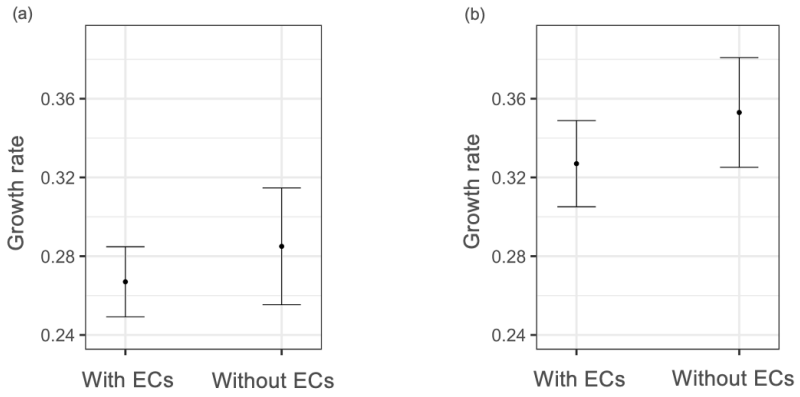

Figure 4.2: Comparison between growth rates of *A. fumigatus* grown with and without epithelial cells for (a) additive noise and (b) multiplicative noise. The error bars indicate the 95% confidence intervals.

4.2 Comparison of fungal strains

A complete pooling model and separate MEMs with additive noise were trained for each fungal strain. The MEM always resulted in a lower information criteria value than the complete pooling model which implies that the MEM is able to generalise to new data better than the complete pooling model (Table 4.3).

Table 4.3: Information criteria values for complete pooling models and mixed effects models for each fungal strain

Strain	**AIC**		**BIC**	
	CP	MEMs	CP	MEMs
MFIG440	17.56	**13.37**	17.67	**13.59**
MFIG441	19.25	**12.47**	19.36	**12.68**
MFIG442	19.69	**13.79**	19.80	**14.00**
MFIG443	20.17	**11.80**	20.28	**12.01**
MFIG444	18.03	**12.16**	18.13	**12.37**
MFIG445	25.47	**17.81**	25.59	**18.04**
MFIG446	29.53	**20.07**	29.65	**20.31**
MFIG447	25.55	**17.02**	25.66	**17.25**
MFIG448	18.96	**11.40**	19.07	**11.61**
MFIG449	17.93	**13.30**	18.03	**13.51**
A. fumigatus	12.87	**10.10**	12.96	**10.27**

Cross validation was then used to estimate the prediction error of the complete pooling model, the separate MEMs, and the multilevel MEM with additive noise when predicting growth of a new strain. The multilevel MEM resulted in the lowest CV error (Table 4.4). The standard deviation of the CV error is high because there is only one fungal strain for the species *A. fumigatus*. Thus, when *A. fumigatus* growth was used as the testing set, the prediction error is very high. The CV error when *A. fumigatus* was excluded from the dataset was also calculated and there was a decrease by a factor of approximately 10.

Table 4.4: Information criteria values of three models. The CV error is reported with its standard deviation. [1]All three species are in the dataset. [2]*A. fumigatus* is excluded from the dataset. Boxplots of the CV error are shown in Appendix B.

Model	AIC	BIC	CV error[1]	CV error[2]
CP	225.03	226.20	20.99 ± 58.28	2.57 ± 0.69
Separate MEMs	153.30	155.64	18.51 ± 50.47	2.55 ± 0.50
Multilevel MEM	168.26	169.04	$\mathbf{0.15 \pm 0.29}$	$\mathbf{0.05 \pm 0.02}$

Unlike the complete pooling model and the separate MEMs, the multilevel mixed effects model is able to account for variations from different groupings in the data which allows for better generalisation (Strains: Figure 4.3, and Replicates: Figure 4.4).

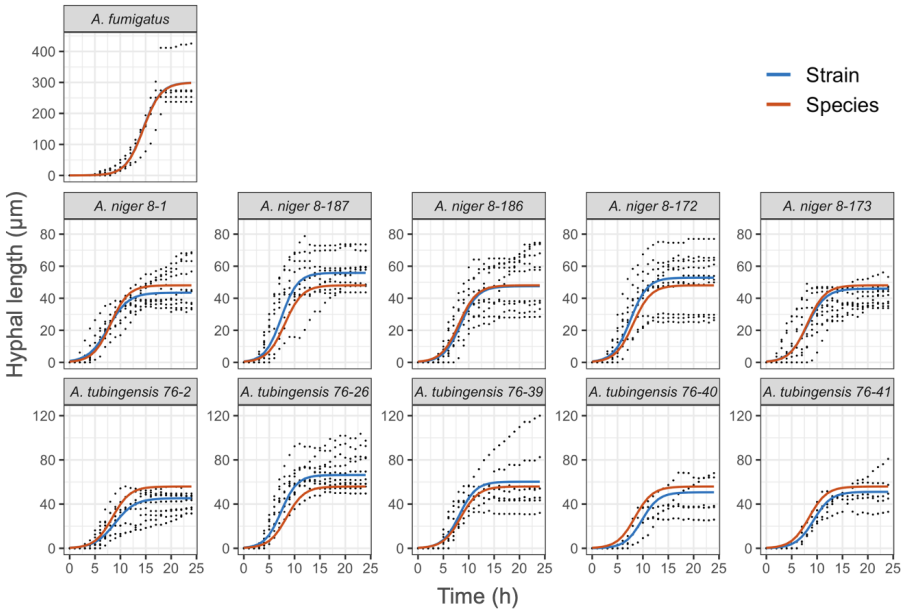

Figure 4.3: Multilevel MEM fits showing variability of the strains within the same species

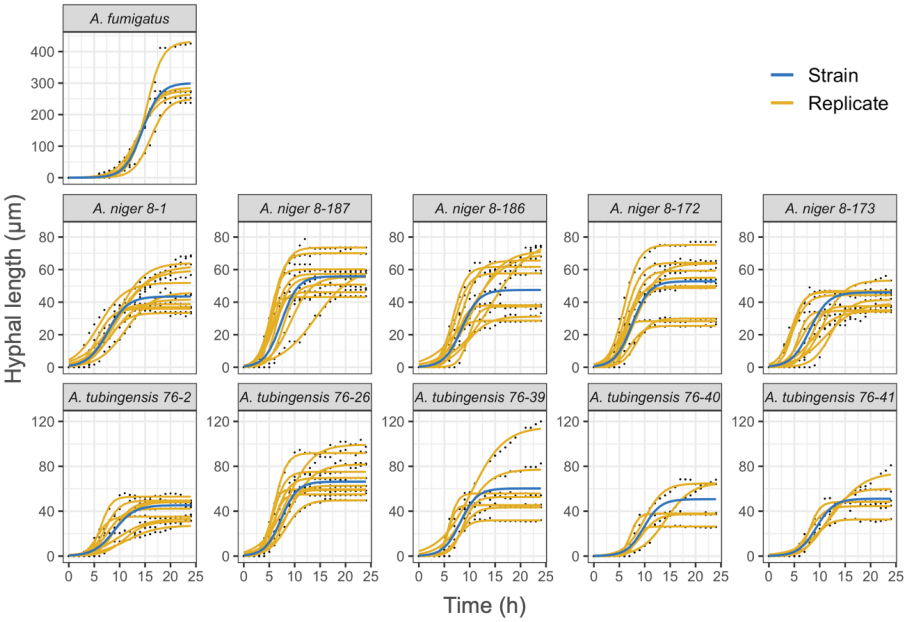

Figure 4.4: Multilevel MEM fits showing variability of the replicates within the same strain

Parameters of the multilevel MEM are given in Appendix C, the maximal growth rates for all strains are given in Appendix D, and significance testing for all strains are given in Appendix E.

Several significant differences were found between the maximal growth rates of the *Aspergillus* strains at the Bonferroni corrected 0.05 significance level, $\alpha_c = 0.05/45$, with *A. fumigatus* having the highest maximal growth rate (Figure 4.5). Additionally, the maximal growth rates of all the *Aspergillus* species are significantly different from one another with that of *A. fumigatus* being the largest (43.39 ± 2.92 for *A. fumigatus*, 8.09 ± 1.05 for *A. tubingensis* and 6.95 ± 0.91 for *A. niger*). This is not surprising since different fungal species are expected to have different growth rates. Furthermore, *A. fumigatus* having the highest maximal growth rate implies that the maximal growth rate is a virulence factor that is indicative of prevalence in IA.

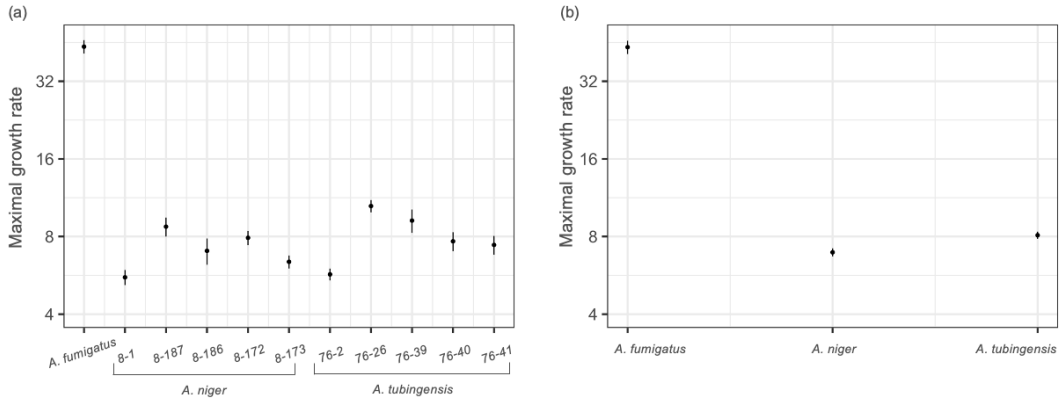

Figure 4.5: Maximal growth rates obtained for (a) 11 *Aspergillus* strains belonging to (b) 3 *Aspergillus* species shown with the 95% confidence intervals on a log scale

5 Discussion

No significant difference was found between the growth rates of the mixed effects model for *A. fumigatus* grown with and without epithelial cells at the 0.05 significance level (p=0.15). Several maximal growth rates of the 11 fungal strains studied were significantly different from each other at the Bonferroni corrected 0.05 significance level, and the maximal growth rates of all 3 fungal species studied were significantly different from one another, with that of *A. fumigatus* being the largest (43.39 ± 2.92 for *A. fumigatus*, 8.09 ± 1.05 for *A. tubingensis* and 6.95 ± 0.91 for *A. niger*).

Paris et al. (1997) were the first to show that *A. fumigatus* condia are engulfed by

pulmonary epithelial cells [21], and a more recent study conducted by Richard et al. (2018) demonstrated that bronchial epithelial cells inhibit *A. fumigatus* conidia germination. The lack of significance for growth rates of *A. fumigatus* grown with and without epithelial cells in this study suggests that epithelial cells only inhibit *A. fumigatus* conidia germination, but not hyphal growth.

A complete pooling model, separate MEMs, and a multilevel MEM were used to model the fungal growth of 11 *Aspergillus* strains belonging to 3 *Aspergillus* species. The multilevel MEM resulted in the lowest CV error which suggests that it has the best generalisation among the three models. The results suggest that MEMs should be used when there are inherent groupings in the data, since variations between elements of the group can be accounted for better. Furthermore, when there are nested groupings in the data, a multilevel MEM is most suitable for modelling fungal growth.

Using the maximum growth rates from the multilevel MEM, significant differences were found for different *Aspergillus* strains and species. In particular, the maximum growth rate of *A. fumigatus* is approximately 5 times and 6 times higher than the maximum growth rates of *A. tubingensis* and *A. niger* respectively. The results suggest that the maximum growth rate is a virulence factor indicative of prevalence in IA, which would support the well-established fact that *A. fumigatus* is the most prevalent species in IA [9][11][22]. However, since there is no gold standard for the virulence ranking of different *Aspergillus* strains and species, a rank correlation test could not be performed to determine whether there is a relationship between maximum fungal growth rates and virulence. In this study, only growth of one fungal strain in the species *A. fumigatus* was collected, whereas *A. niger* and *A. tubingensis* had 5 fungal strains each. More data for strains belonging to *A. fumigatus* can be collected to obtain more accurate growth rate estimates of this species.

A logistic growth model was used in this study to model hyphal growth, however, one criticism is that due to the symmetrical nature of the logistic model, it is unlikely to model the lag phase of fungal growth well. Alternate growth models have been proposed which have more parameters to account for the lag phase of growth better. For instance, Mavridou et al. suggested modelling the growth process as a piecewise function where y is the hyphal length, y_0 is the hyphal length after the lag phase, τ is the duration of the lag phase, v is the growth rate, and λ is the growth decay constant (Equation 14, Figure 5.1) [23].

$$y(t) = \begin{cases} y_0 & 0 \leq t < \tau \\ (y_0 + v(t-\tau))\mathrm{e}^{-\lambda(t-\tau)} & t \geq \tau \end{cases} \tag{14}$$

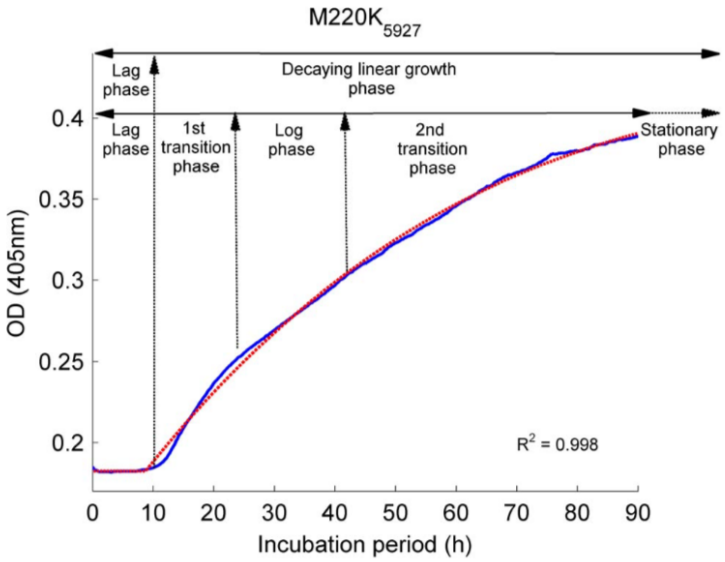

Figure 5.1: Growth model proposed by Mavridou et al. [23]

Similarly, Baranyi et al. proposed a model with more parameters to account for the lag phase of growth better where y is the hyphal length, y_0 is the hyphal length at time $t = 0$, y_{max} is the maximum hyphal length, m is the Richard's curvature parameter after the exponential phase, n is the curvature parameter after the lag phase, g is the maximum hyphal growth rate, λ is the duration of lag, and s is an integral variable. (Equation 15, Figure 5.2) [24].

$$y(t) = y_0 + g\,A_n(t) - \frac{1}{m}\ln\left(1 + \frac{e^{m\,g\,A_n(t)} - 1}{e^{m(y_{max} - y_0)}}\right) \tag{15}$$

$$A_n(t) = \int_0^t \frac{s^n}{\lambda^n + s^n} ds$$

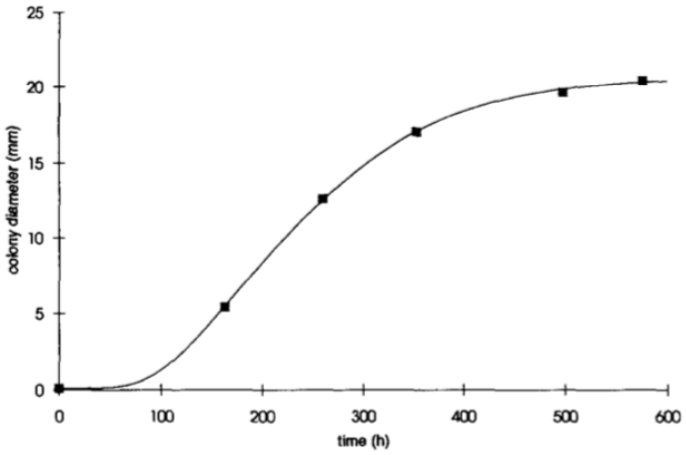

Figure 5.2: Growth model proposed by Baranyi et al. [24]

One problem with the alternate models it that there is an increase in the number of model parameters. The model proposed by Mavridou et al. has 4 parameters while the model proposed by Baranyi et al. has 6 parameters. Information criteria values can help in determining whether there is a positive trade-off between a decrease in squared error and an increase in model complexity, however, this remains unexplored.

References

[1] Brahm H. Segal and Thomas J. Walsh. "Current approaches to diagnosis and treatment of invasive aspergillosis". In: *American Journal of Respiratory and Critical Care Medicine* 173.7 (2006), pp. 707–717. ISSN: 1073449X. DOI: 10.1164/rccm.200505-727SO.

[2] Jean Paul Latgé et al. "Aspergillus fumigatus: Growth and virulence". In: *Journal of Medical Microbiology* 23.3 (2009), pp. 174–179. ISSN: 13693786. DOI: 10.1128/jb.109.3.1097-1100.1972.

[3] David W. Denning. "Therapeutic outcome in invasive aspergillosis". In: *Clinical Infectious Diseases* 23.3 (1996), pp. 608–615. ISSN: 10584838. DOI: 10.1093/clinids/23.3.608.

[4] Vijaya R. Bhatt, George M. Viola, and Alessandra Ferrajoli. "Invasive fungal infections in acute leukemia". In: *Therapeutic Advances in Hematology* 2.4 (2011), pp. 231–247. ISSN: 20406215. DOI: 10.1177/2040620711410098.

[5] Sanjay H. Chotirmall et al. "Immunoevasive aspergillus virulence factors". In: *Mycopathologia* 178.5-6 (2014), pp. 363–370. ISSN: 0301486X. DOI: 10.1007/s11046-014-9768-y.

[6] Matteo Bassetti, Maddalena Peghin, and Antonio Vena. "Challenges and Solution of Invasive Aspergillosis in Non-neutropenic Patients: A Review". In: *Infectious Diseases and Therapy* 7.1 (2018), pp. 17–27. ISSN: 21936382. DOI: 10.1007/s40121-017-0183-9. URL: https://doi.org/10.1007/s40121-017-0183-9.

[7] Carolina Garcia-Vidal et al. "Causes of death in a contemporary cohort of patients with invasive aspergillosis". In: *PLoS ONE* 10.3 (2015), pp. 1–10. ISSN: 19326203. DOI: 10.1371/journal.pone.0120370.

[8] Georg Maschmeyer, Antje Haas, and Oliver A. Cornely. "Invasive aspergillosis: Epidemiology, diagnosis and management in immunocompromised patients". In: *Drugs* 67.11 (2007), pp. 1567–1601. ISSN: 00126667. DOI: 10.2165/00003495-200767110-00004.

[9] Jean Paul Latgé and Georgios Chamilos. "Aspergillus fumigatus and aspergillosis in 2019". In: *Clinical Microbiology Reviews* 33.1 (2020), pp. 310–350. ISSN: 10986618. DOI: 10.1128/CMR.00140-18.

[10] Jeffrey D. Jenks and Martin Hoenigl. "Treatment of aspergillosis". In: *Journal of Fungi* 4.3 (2018), pp. 1–17. ISSN: 2309608X. DOI: 10.3390/jof4030098.

[11] Judith C. Rhodes. "Aspergillus fumigatus: Growth and virulence". In: *Medical Mycology* 44.SUPPL. 1 (2006), pp. 77–81. ISSN: 13693786. DOI: 10.1080/13693780600779419.

[12] Frank L. Van De Veerdonk et al. "Aspergillus fumigatus morphology and dynamic host interactions". In: *Nature Reviews Microbiology* 15.11 (2017), pp. 661–674. ISSN: 17401534. DOI: 10.1038/nrmicro.2017.90. URL: http://dx.doi.org/10.1038/nrmicro.2017.90.

[13] Nir Osherov. "Interaction of the pathogenic mold Aspergillus fumigatus with lung epithelial cells". In: *Frontiers in Microbiology* 3.SEP (2012), pp. 1–9. ISSN: 1664302X. DOI: 10.3389/fmicb.2012.00346.

[14] Célimène Galiger et al. "Assessment of efficacy of antifungals against Aspergillus fumigatus: Value of real-time bioluminescence imaging". In: *Antimicrobial Agents and Chemotherapy* 57.7 (2013), pp. 3046–3059. ISSN: 00664804. DOI: 10.1128/AAC.01660-12.

[15] Neil A. R. Gow and Geoffrey M. Gadd. "JOIN US ON THE INTERNET VIA WWW , GOPHER , FTP OR EMAIL : THE GROWING Edited by". In: (1995), p. 478.

[16] Ricardo Araujo and Acacio Gonçalves Rodrigues. "Variability of germinative potential among pathogenic species of Aspergillus". In: *Journal of Clinical Microbiology* 42.9 (2004), pp. 4335–4337. ISSN: 00951137. DOI: 10.1128/JCM.42.9.4335-4337.2004.

[17] Derek Paisley, Geoffrey D. Robson, and David W. Denning. "Correlation between in vitro growth rate and in vivo virulence in Aspergillus fumigatus". In: *Medical Mycology* 43.5 (2005), pp. 397–401. ISSN: 13693786. DOI: 10.1080/13693780400005866.

[18] Nicolas Richard et al. "Human Bronchial Epithelial Cells Inhibit Aspergillus fumigatus Germination of Extracellular Conidia via FleA Recognition". In: *Scientific Reports* 8.1 (2018), pp. 1–11. ISSN: 20452322. DOI: 10.1038/s41598-018-33902-0.

[19] Chris D. Lauruschkat, Hermann Einsele, and Juergen Loeffler. "Immunomodulation as a therapy for Aspergillus infection: Current status and future perspectives". In: *Journal of Fungi* 4.4 (2018), pp. 1–17. ISSN: 2309608X. DOI: 10.3390/jof4040137.

[20] A. Caroli and G.B. Frisoni. "The dynamics of Alzheimer's disease biomarkers in the Alzheimer's Disease Neuroimaging Initiative cohort". In: *Neurobiology of Aging* 31.8 (Aug. 2010), pp. 1263–1274. ISSN: 01974580. DOI: 10.1016/j.neurobiolaging.2010.04.024. URL: https://linkinghub.elsevier.com/retrieve/pii/S0197458010001892.

[21] S Paris et al. "Internalization of Aspergillus fumigatus conidia by epithelial and endothelial cells". In: *Infection and Immunity* 65.4 (Apr. 1997), pp. 1510–1514. ISSN: 0019-9567. DOI: 10.1128/iai.65.4.1510-1514.1997. URL: https://journals.asm.org/doi/10.1128/iai.65.4.1510-1514.1997.

[22] Thorsten Heinekamp et al. “Interference of Aspergillus fumigatus with the immune response”. In: *Seminars in Immunopathology* 37.2 (2015), pp. 141–152. ISSN: 18632300. DOI: 10.1007/s00281-014-0465-1.

[23] Eleftheria Mavridou et al. “Composite Survival Index to Compare Virulence Changes in Azole-Resistant Aspergillus fumigatus Clinical Isolates”. In: *PLoS ONE* 8.8 (2013), pp. 1–11. ISSN: 19326203. DOI: 10.1371/journal.pone.0072280.

[24] József Baranyi and Terry A. Roberts. “A dynamic approach to predicting bacterial growth in food”. In: *International Journal of Food Microbiology* 23.3-4 (1994), pp. 277–294. ISSN: 01681605. DOI: 10.1016/0168-1605(94)90157-0.

Appendix

A Fungal strains and species used in the study

Table A: Fungal strains and species used in the study

Strain	Scientific name	Strain	Scientific name
A. fumigatus	-	-	-
MFIG440	*A. niger* 8-1	MFIG445	*A. tubingensis* 76-2
MFIG441	*A. niger* 8-187	MFIG446	*A. tubingensis* 76-26
MFIG442	*A. niger* 8-186	MFIG447	*A. tubingensis* 76-39
MFIG443	*A. niger* 8-172	MFIG448	*A. tubingensis* 76-40
MFIG444	*A. niger* 8-173	MFIG449	*A. tubingensis* 76-41

B Cross validaton errors of the CP and MEMs

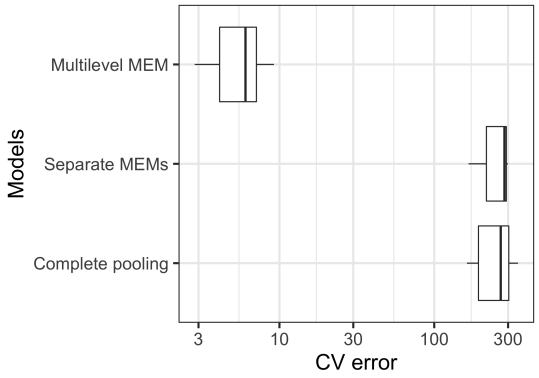

Figure B: Boxplots of the cross validation errors for the complete pooling model, separate MEMs and the multilevel MEMs when predicting growth of a new fungal strain

C Parameters of the multilevel MEM

Table C: Parameters of the multilevel mixed effects model

Parameter	Value	Parameter	Value
A_0	134.48	$\sigma_{\bar{u}}$	7.42
B_0	10.36	$\sigma_{\bar{v}}$	0.79
C_0	1.73	$\sigma_{\bar{w}}$	0.17
$\sigma_{\tilde{u}}$	116.92	σ_u	21.06
$\sigma_{\tilde{v}}$	2.98	σ_v	2.01
$\sigma_{\tilde{w}}$	0.0026	σ_w	0.75
$\sigma(\epsilon)$	3.38		

D Maximal growth rates of all fungal strains

Table D: Maximal growth rates of all fungal strains with the 95% confidence intervals

Rank	Strain	Maximal growth rate
1	*A. fumigatus*	42.86 ± 2.21
2	MFIG446	11.33 ± 0.63
3	MFIG441	9.63 ± 0.87
4	MFIG447	9.60 ± 0.97
5	MFIG443	8.74 ± 0.59
6	MFIG448	7.97 ± 0.71
7	MFIG449	7.20 ± 0.58
8	MFIG442	6.86 ± 0.72
9	MFIG444	6.13 ± 0.41
10	MFIG440	4.99 ± 0.29
11	MFIG445	4.85 ± 0.26

E Significance testing of maximal growth rates of all fungal strains

Table E: Significance testing of the maximal growth rates of 11 *Aspergillus* strains at the Bonferroni corrected 0.05 significance level. The row and column headings are the strains arranged in order of descending maximum growth rate.

Strain number	6	1	7	3	8	9	2	4	0	5
10										
6										
1										
7										
3										
8										
9										
2										
4										
0										